



## Calhoun: The NPS Institutional Archive DSpace Repository

---

Theses and Dissertations

1. Thesis and Dissertation Collection, all items

---

1979-06

### Experimental FLIR study

Gruber, James Powell

Monterey, California. Naval Postgraduate School

---

<http://hdl.handle.net/10945/18719>

---

This publication is a work of the U.S. Government as defined in Title 17, United States Code, Section 101. Copyright protection is not available for this work in the United States.

*Downloaded from NPS Archive: Calhoun*



<http://www.nps.edu/library>

Calhoun is the Naval Postgraduate School's public access digital repository for research materials and institutional publications created by the NPS community.

Calhoun is named for Professor of Mathematics Guy K. Calhoun, NPS's first appointed -- and published -- scholarly author.

**Dudley Knox Library / Naval Postgraduate School  
411 Dyer Road / 1 University Circle  
Monterey, California USA 93943**

EXPERIMENTAL FLIR STUDY

James Powell Gruber



# NAVAL POSTGRADUATE SCHOOL

## Monterey, California



# THESIS

EXPERIMENTAL FLIR STUDY

by

James Powell Gruber

June, 1979

Thesis Advisor:

E. C. Crittenden Jr.

Approved for public release; distribution unlimited

T187332



**Unclassified**

SECURITY CLASSIFICATION OF THIS PAGE (When Data Entered)

<b>REPORT DOCUMENTATION PAGE</b>		<b>READ INSTRUCTIONS BEFORE COMPLETING FORM</b>
1. REPORT NUMBER	2. GOVT ACCESSION NO.	3. RECIPIENT'S CATALOG NUMBER
4. TITLE (and Subtitle) Experimental FLIR Study		5. TYPE OF REPORT & PERIOD COVERED Master's Thesis; June, 1979
7. AUTHOR(s) James Powell Gruber		6. PERFORMING ORG. REPORT NUMBER
9. PERFORMING ORGANIZATION NAME AND ADDRESS Naval Postgraduate School Monterey, California 93940		10. PROGRAM ELEMENT, PROJECT, TASK AREA & WORK UNIT NUMBERS
11. CONTROLLING OFFICE NAME AND ADDRESS Naval Postgraduate School Monterey, California 93940		12. REPORT DATE June, 1979
14. MONITORING AGENCY NAME & ADDRESS (if different from Controlling Office) Naval Postgraduate School Monterey, California 93940		13. NUMBER OF PAGES 79
16. DISTRIBUTION STATEMENT (of this Report) Approved for public release; distribution unlimited		15. SECURITY CLASS. (of this report) Unclassified
		16a. DECLASSIFICATION/DOWNGRADING SCHEDULE
17. DISTRIBUTION STATEMENT (of the abstract entered in Block 20, if different from Report) Approved for public release; distribution unlimited		
18. SUPPLEMENTARY NOTES		
19. KEY WORDS (Continue on reverse side if necessary and identify by block number) NPS FLIR		
20. ABSTRACT (Continue on reverse side if necessary and identify by block number) A single cell, serially scanned, thermal imaging FLIR system has been constructed at NPS Monterey. The system consisted of a Cassegrain type reflecting telescope with a convergent beam, oscillating mirror scan system and HgCdTe and InSb single cell infrared detectors. The system was first tested using visible light and then switched to the infrared wavelengths. The FLIR has imaged scenes with a temperature difference of 90K above ambient. MTF measurements have shown it to be diffraction		



20. cont.:

limited by the active area of the detector crystal and the optics.



Approved for public release; distribution unlimited

Experimental FLIR Study

by

James Powell Gruber  
Lieutenant, United States Navy  
B.S.S.E., United States Naval Academy, 1973

Submitted in partial fulfillment of the  
requirement for the degree of

MASTER OF SCIENCE IN PHYSICS

from the

NAVAL POSTGRADUATE SCHOOL  
June, 1979

Thesis  
G86095  
c.1

## ABSTRACT

A single cell, serially scanned, thermal imaging FLIR system has been constructed at NPS Monterey. The system consisted of a Cassegrain type reflecting telescope with a convergent beam, oscillating mirror scan system, and HgCdTe and InSb single cell infrared detectors. The system was first tested using visible light and then switched to the infrared wavelengths. The FLIR has imaged scenes with a temperature difference of 9°K above ambient. MTF measurements have shown it to be diffraction limited by the active area of the detector crystal and the optics.



TABLE OF CONTENTS

	<u>PAGE</u>
I. INTRODUCTION . . . . .	9
II. BACKGROUND . . . . .	11
III. DESIGN STEPS . . . . .	13
A. OPTICS . . . . .	13
1. Parabolic Off-Axis Mirror . . . . .	13
2. Cassegrain Optics . . . . .	16
B. SCANNING SYSTEM . . . . .	17
1. Parallel vs. Convergent Beam Scan . .	20
2. Raster . . . . .	28
C. DETECTORS . . . . .	29
D. ELECTRONICS . . . . .	34
1. Mirror Scan Drive . . . . .	34
2. Detector/Video . . . . .	36
IV. RESULTS . . . . .	41
A. VISIBLE . . . . .	41
B. INFRARED . . . . .	47
C. MTF CALCULATIONS . . . . .	56
V. SUMMARY . . . . .	64
VI. AREAS FOR FURTHER STUDY . . . . .	65
APPENDIX A ENERGY CALCULATIONS . . . . .	68
APPENDIX B SYSTEM PHOTOGRAPHS . . . . .	71
APPENDIX C OPERATING INSTRUCTIONS . . . . .	75
BIBLIOGRAPHY . . . . .	78
INITIAL DISTRIBUTION LIST . . . . .	79



## LIST OF FIGURES

	<u>PAGE</u>
1. Parabolic Off-Axis Mirror . . . . .	15
2. Focal Point Location . . . . .	15
3. Dahl-Kirkham Astronomical Telescope . . . . .	18
4. Type (i) Mirror Frequency Response . . . . .	21
5. Type (i) Mirror Frequency Response . . . . .	22
6. Type (ii) Mirror Frequency Response . . . . .	23
7. Type (ii) Mirror Frequency Response . . . . .	24
8. "Parallel" Beam Scanning System . . . . .	25
9. Convergent Beam Scanning System . . . . .	27
10. Convergent Scan Defocusing . . . . .	27
11. HgCdTe Detector Characteristics . . . . .	30
12. InSb Detector Characteristics . . . . .	31
13. Silicon Avalanche Diode Characteristics . . . . .	32
14. InSb Internal Resistance . . . . .	37
15. Circuit for Avalanche Detector . . . . .	38
16. Circuit for InSb Photovoltaic Cells . . . . .	38
17. Circuit for HgCdTe Photoconductive Cells . . . . .	38
18. Visible Light Target . . . . .	42
19. First Visible Light Image . . . . .	43
20. Visible Light Target at 64 Meters . . . . .	43
21. Target Using .034 cm Pinhole . . . . .	45
22. Target Using .053 cm Pinhole . . . . .	45
23. Target Using 3 Hz Slow Scan . . . . .	46



	<u>PAGE</u>
24. Target Using .5 Hz Slow Scan . . . . .	46
25. Infrared Targets . . . . .	49
26. First Infrared Images . . . . .	50
27. Infrared Images with Installed Pinhole . . . . .	50
28. Infrared Targets at 64 Meters, HgCdTe . . . . .	52
29. Infrared Targets at 32.6 Meters, HgCdTe . . . . .	52
30. Infrared Target at 32.6 Meters, HgCdTe . . . . .	53
31. InSb Detector Impedence Mismatch . . . . .	53
32. Infrared Images with Disconnected Pulser . . . . .	55
33. Corrected Images, HgCdTe . . . . .	55
34. Nichrome Wire MTF Target . . . . .	57
35. Single Wire Delta Response . . . . .	58
36. Enlarged Single Wire Response . . . . .	58
37. Theoretical Pinhole MTF . . . . .	60
38. Theoretical Optics MTF . . . . .	61
39. Comparison of Experimental and Theoretical MTF .	62
40. Infrared Image of MTF Target . . . . .	63
41. System MTF Response . . . . .	63
42. Optics and Scan Systems . . . . .	71
43. Electronics . . . . .	72
44. Scan Mirrors . . . . .	73
45. Scan Mirrors and Detector in Dewar . . . . .	74



## ACKNOWLEDGEMENT

I wish to express my appreciation to Professors Milne and Rodenback for their assistance with the computer programs and detector electronics respectively.

I wish to acknowledge the invaluable assistance of Mr. Robert Moeller who manufactured the mechanical structures of the system and Mr. Ken Smith for his advice on the electronics components.

I would like to specially thank Professor Crittenden whose wisdom, guidance and inspiration made this thesis possible.

I would finally like to thank my wife, Roseann, for her patience and understanding; they were as important to the completion of this thesis as any other factor.



## I. INTRODUCTION

FLIR, or Forward Looking InfraRed, is a device designed to detect the thermal differences in remote objects, utilizing that portion of the electromagnetic spectrum commonly known as heat, displaying these differences as images visible to the human eye. The advantages of the infrared wavelengths lie in their increased ability to penetrate atmospheric aerosols and to detect emissions from objects above or below the ambient background temperature. Since man and his machines constantly produce heat as a by-product, night is no longer a cloak of concealment. Other sources of temperature difference also act as sources, such as differences in past sun illumination, water temperatures, etc.

The basic idea behind the FLIR is not new. The earliest system was a circa-1930 Evaporagraph. This was extremely limited due to inherent insensitivity and time response problems.

The ability to create real time thermal images, however, had to wait for the development of sensitive, fast response-time infrared detectors. This occurred in the late 1950's and the modern FLIR was born.

Since then, the advance of solid state physics and the advent of tri-metal detectors, such as HgCdTe or



SnPbTe which require less extreme cooling, have further stimulated the application of these devices.



## II. BACKGROUND

Since their inception in the late 1950's, FLIRs have gained ever increasing acceptance in military circles. It is, therefore, increasingly important that military officers become familiar with design, operating principles and limitations of the FLIR.

While FLIR concepts have been taught at NPS for many years, there has been little opportunity for direct experience with the hardware behind the concepts. This thesis was undertaken as a system for experimental study.

There are several uses to which an operating FLIR can be put at NPS. In addition to the knowledge gained by designing and constructing a FLIR, it can be a stepping stone to understanding the newer technologies of present day FLIRs. Several projects utilizing the infrared wavelengths, such as a recent project in atmospheric turbulence, could also benefit from the availability of a thermal imaging system.

Thermal imaging is accomplished, in a FLIR, as follows. Optics collect, filter and focus the infrared radiation from a scene onto an infrared detector. An optical scanning system moves the image across the detector creating a train of analog electrical signals which are then processed and amplified for display on a video monitor; thus converting the infrared scene into its visible analog.



The design of this FLIR was kept as simple as possible to permit study of the effects of individual components and to utilize those parts already available at NPS Monterey. No other constraints were imposed. Preferably the system would operate over a wide band of wavelengths, exhibit all or most facets of FLIR principles and be capable of modification as the newer technologies become available.



### III. DESIGN STEPS

The first and overriding concern throughout the design and construction of the FLIR system was optimization in terms of components available at NPS Monterey. Due to the broad range of research undertaken at NPS, parts which were adaptable to FLIR use were easily obtained.

It was decided to work the design through first in the visible region of the spectrum. This eased the problems of focus and alignment and allowed an understanding of subsystem interrelations vs. system performance. The initial design had a catoptric front-end optical system with a catadioptric scan system. With the IR lenses being germanium and thus opaque to visible light, it was thought that designing and setting up the system in the visible region first would allow a better understanding of the principles and problems of FLIRs prior to switching to the infrared region.

#### A. OPTICS

##### 1. Parabolic Off-Axis Mirror

The first optical design was the use of an 8.57 cm diameter parabolic off-axis mirror with a focal length of 25.87 cm. This type of mirror was available from earlier use in an infrared spectrometer.



A parabolic off-axis mirror experiences severe distortions for arriving rays which are not parallel with the optic axis. This has the effect of limiting the total system field of view. Due to scanner mirror constraints, the limiting effect of the mirror field of view was not considered important. The constraint which led to this decision is discussed more fully in the section on the parallel beam scanning system.

Another factor in favor of the parabolic off-axis mirror was its lack of central obscuration, which allowed the mirror's total surface area to be considered as the collecting aperture. This means a smaller optics package for a given energy collecting area.

A parabolic off-axis mirror is, in effect, a mirror segment cut from a larger parabolic surface and then mounted, as shown in FIG. (1). Prior to its use, the focal point had to be located.

A HeNe laser beam was run through a beam expander and positioned such that it filled the entire mirror. Theoretically, when the focal point was correctly located the image of the beam would be a small spot. In addition, moving the focal plane away from the focal point, in a line between the mirror and the focal point, will cause the spot to grow larger. This is shown in FIG. (2) column a. Any errors in the location of the mirror focal point will manifest themselves when the circle becomes an ellipse, FIG. (2) column b.



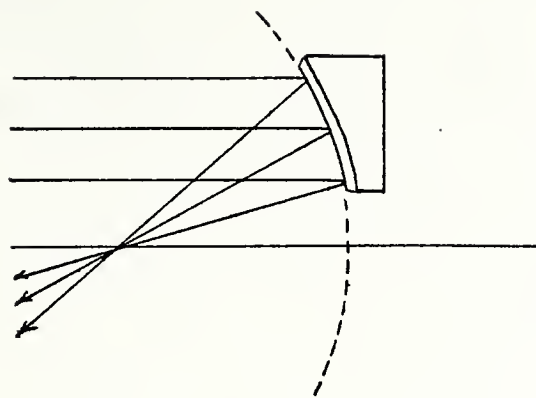


FIG. (1) Parabolic Off-Axis mirror

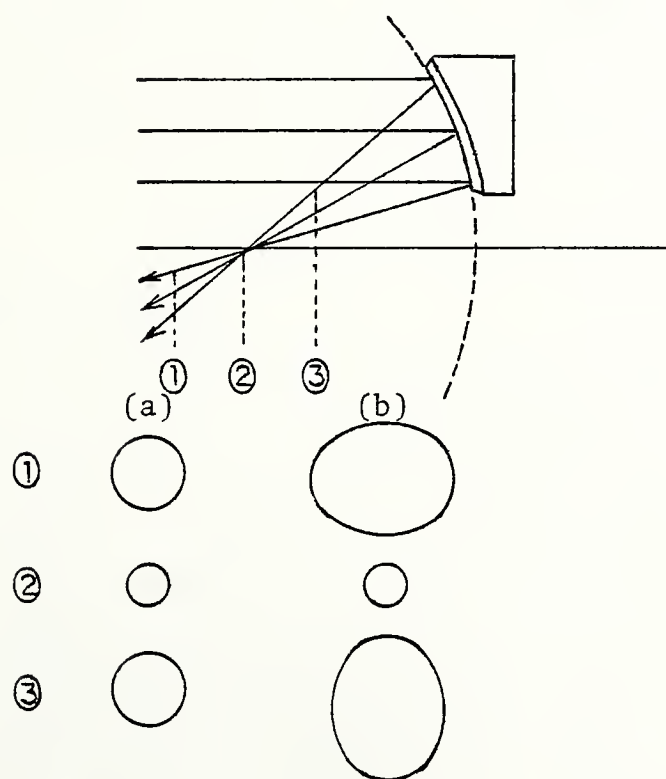


FIG. (2) Focal Point Location



Utilizing this technique quickly located the focal point. Upon attempting to form an image at that point, serious image coma and astigmatism were noted. A closer examination of the mirror brought forth the fact that since the mirror had been cut from a larger mirror segment, the  $f/\#$  was much smaller than it had at first seemed. The focal point was located 2.54 cm below a line normal to the mirror face and tangent to its lower edge. This means that the minimum diameter of the mirror from which the segment had been cut was 22.2 cm. With a focal length of 25.87 cm, the  $f/\#$  is 1.16. While this was acceptable when the mirror segment was used in an IR Spectrograph, the small  $f/\#$  was causing aberrations and image degradation for objects being viewed which were not directly on the optic axis. It was decided to try a more conventional optical telescope.

## 2. Cassegrain Optics

It became apparent that the parabolic off-axis mirror was not suited to the task and a 15.24 cm diameter Cassegrainian type reflecting astronomical telescope with an equivalent focal length of 228.6 cm was substituted.

The Cassegrainian type telescope is a central obscuration type utilizing an adjustable spherical primary mirror and a fixed ellipsoidal secondary. This type of telescope is called a Dahl-Kirkham and is shown in FIG. (3).



Several of the advantages of the Dahl-Kirkham telescope are:

- a. It was already assembled and aligned.
- b. The 15.24 cm aperture is a large collecting surface which offsets the central obscuration.
- c. It is catoptric.
- d. Mounting hardware for the scanning system is already attached in the form of an eyepiece screw fitting.

Its disadvantages are minor. The larger size and central obscuration, not being design parameters, are acceptable.

The Dahl-Kirkham telescope is the finalized front end optical system.

## B. SCANNING SYSTEM

Concurrent with the design of the front-end optics was the consideration of the scanning system. Since the scan system design is not critically dependent upon the input optics, the two efforts ran simultaneously. A number of options present themselves at this point; however, any decision on the scanning system also has to take into account such other areas as display, image recognition vs. the human eye and detector types.



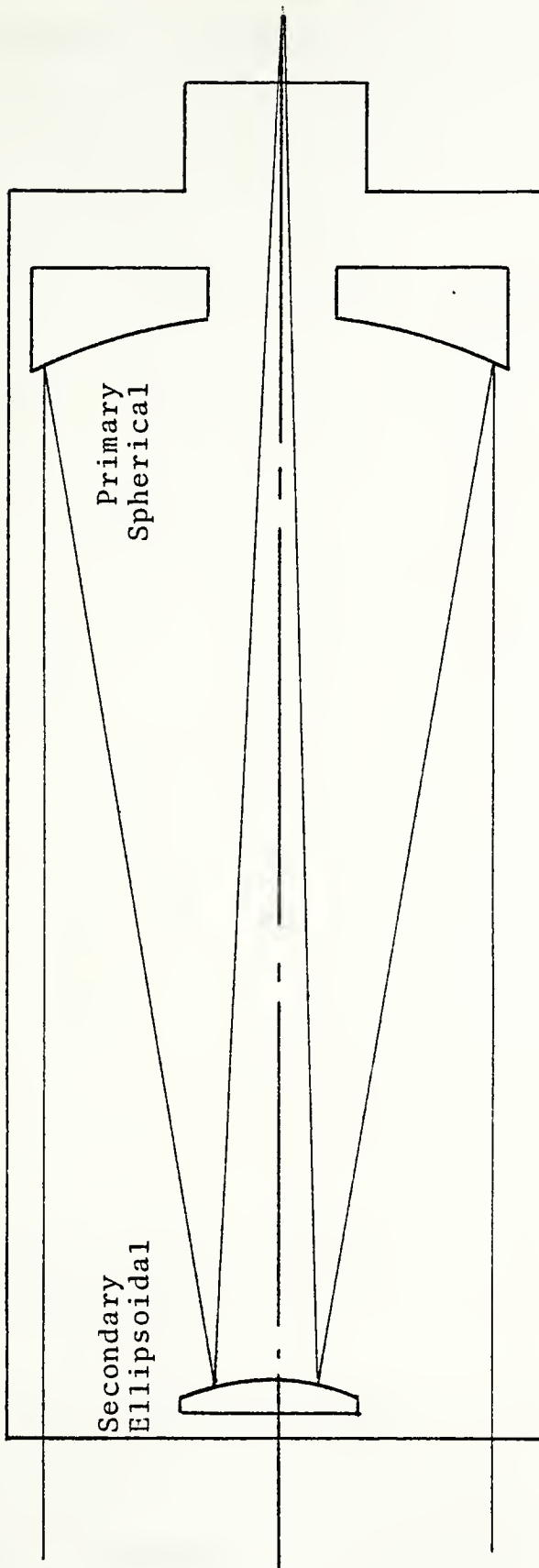


FIG. (3) Dahl-Kirkham Astronomical Telescope



The detector's input to the scanning system is simple due to the fact that there are only single cell detectors available. Without linear or planar arrays, the scan must be two dimensional.

With any device the ultimate use will drive the design. In the case of the FLIR, its ultimate purpose is to present a visible picture to a human operator. It is, therefore, desirable to try to optimize the FLIR display in relation to known characteristics of the human eye. Chapter 4 of Reference 1 contains an interesting and thorough discussion of the subject of visual psychophysics as related to screen viewing. Any attempt to optimize for the human factor must take into account the information so presented. The human interface was not normally considered; however, wherever a design parameter was amenable to change, the change was made in favor of the human element.

Given the amount of knowledge and experience resident in modern television technology, the ideal scan system should be TV compatible. TABLE (I) below lists some of the characteristics of the standard U.S. television raster.

Line Repetition Frequency -----	15750 Hz
Frame Rate -----	1/30 Sec
Interlaced Fields -----	Yes
Blanking Time -----	10 uSec/Line 1000uSec/Frame
Line Utilization Factor -----	.7
Total Resolution Elements -----	147,000

---

TABLE (I) Standard U.S. Television Raster

Many FLIRs of today are TV compatible; however, the high scan speeds required rule out several types of scan systems, including those that depend on oscillating mirrors.



The scanning devices on hand are several oscillating plane mirrors manufactured by General Scanning, Inc. The mirrors consist of two types: (i) position feedback and (ii) nonfeedback. The feedback type mirror returns an error signal to a control device which is used to increase or decrease drive motor power. The feedback mirror is then able to follow an arbitrary (non sinusoidal) signal to a high (relative) frequency. This fact makes it the choice for the fast scan dimension of the system. In contrast, the nonfeedback type mirror is limited much more in its frequency response range for nonsinusoidal signals. This means that it can be used for the slow scan dimension of the system. Figures (4-7) contain plots of mirror response as a function of input signal amplitude for various sinusoidal frequencies.

### 1. Parallel vs. Convergent Beam Scan

There are two general types of scan technique, parallel beam and convergent beam.

In parallel beam scanning, the scan system is located in a region where the images are "afocal." This technique avoids image blurring caused by focal point shifting. A field lens located in front of the detector intercepts the "afocal" beam and focuses it upon the detector as shown in FIG. (8).

In convergent beam scanning, the scan mirrors are located between the optics and the focal plane as shown



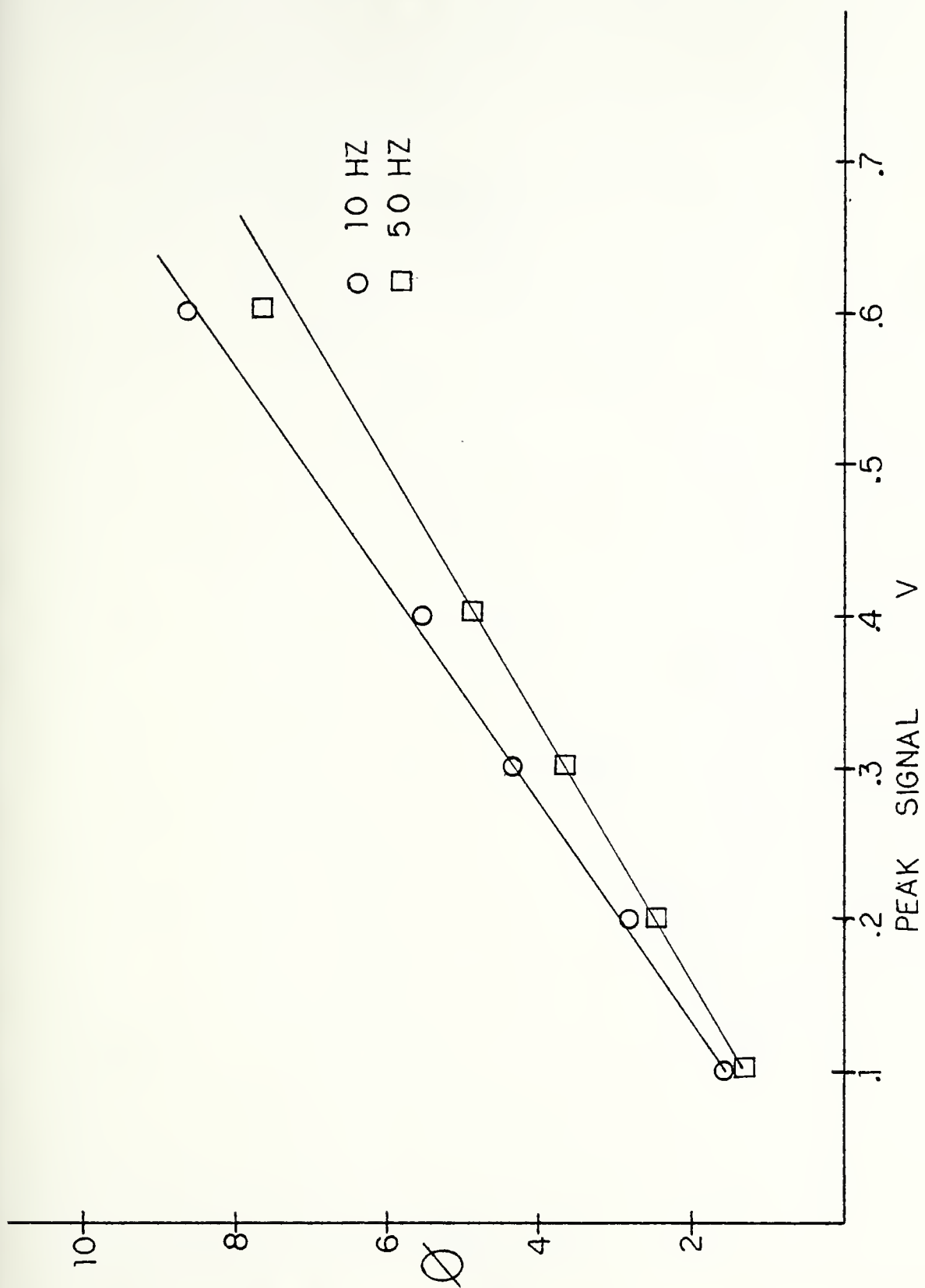


FIG. (4) Type (i) Mirror Frequency Response



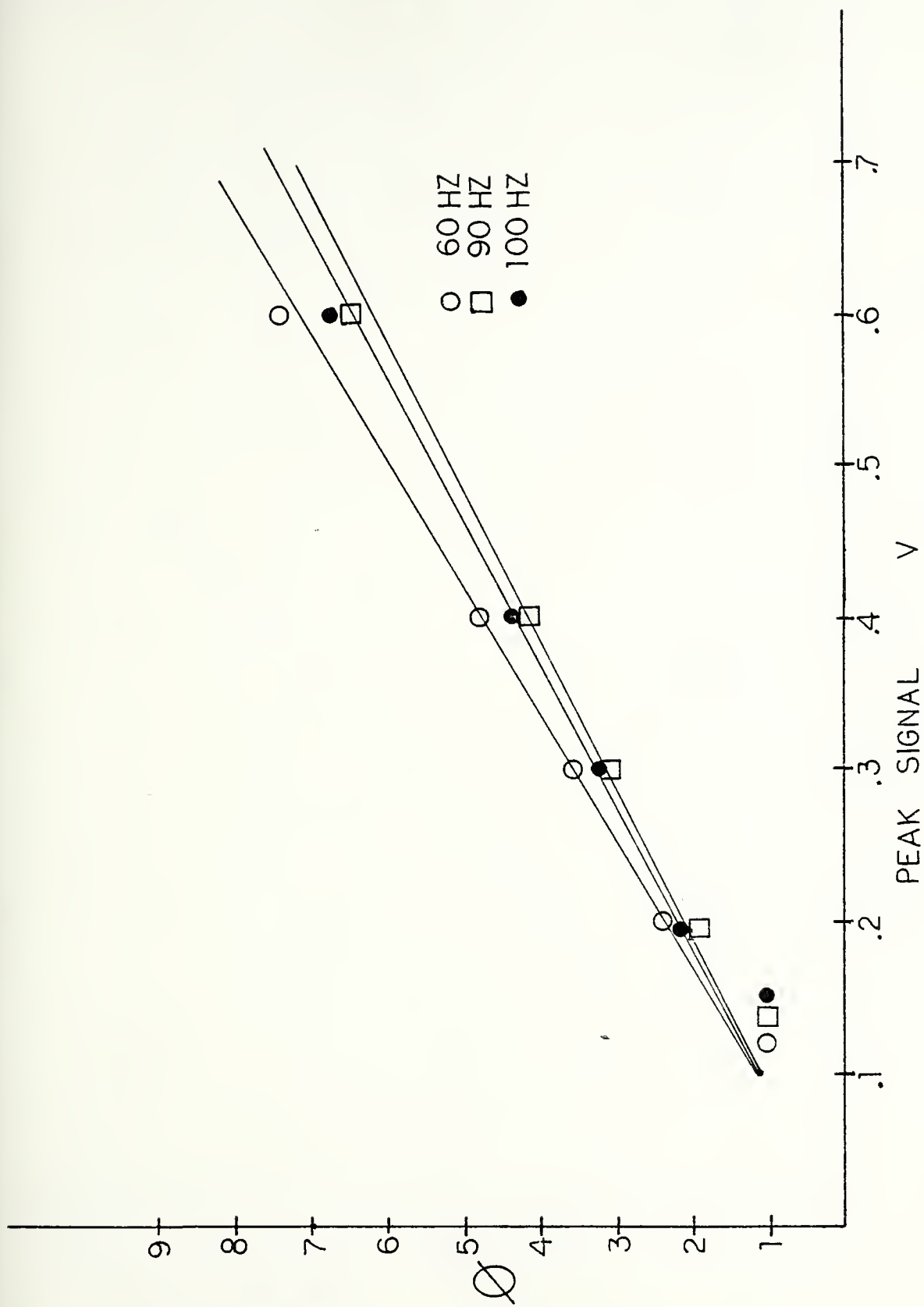


FIG. (5) Type (i) Mirror Frequency Response



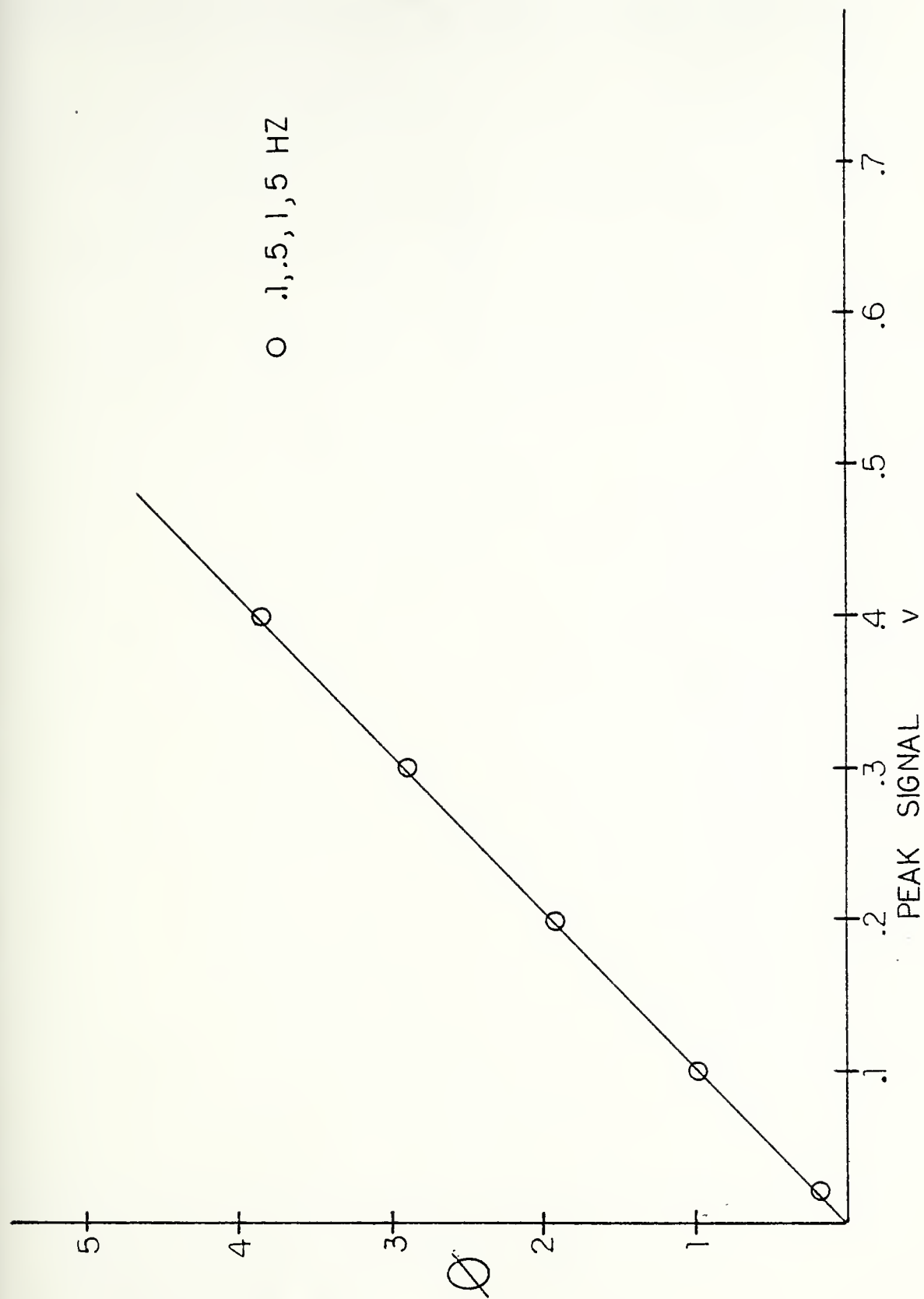


FIG. (6) Type (ii) Mirror Frequency Response



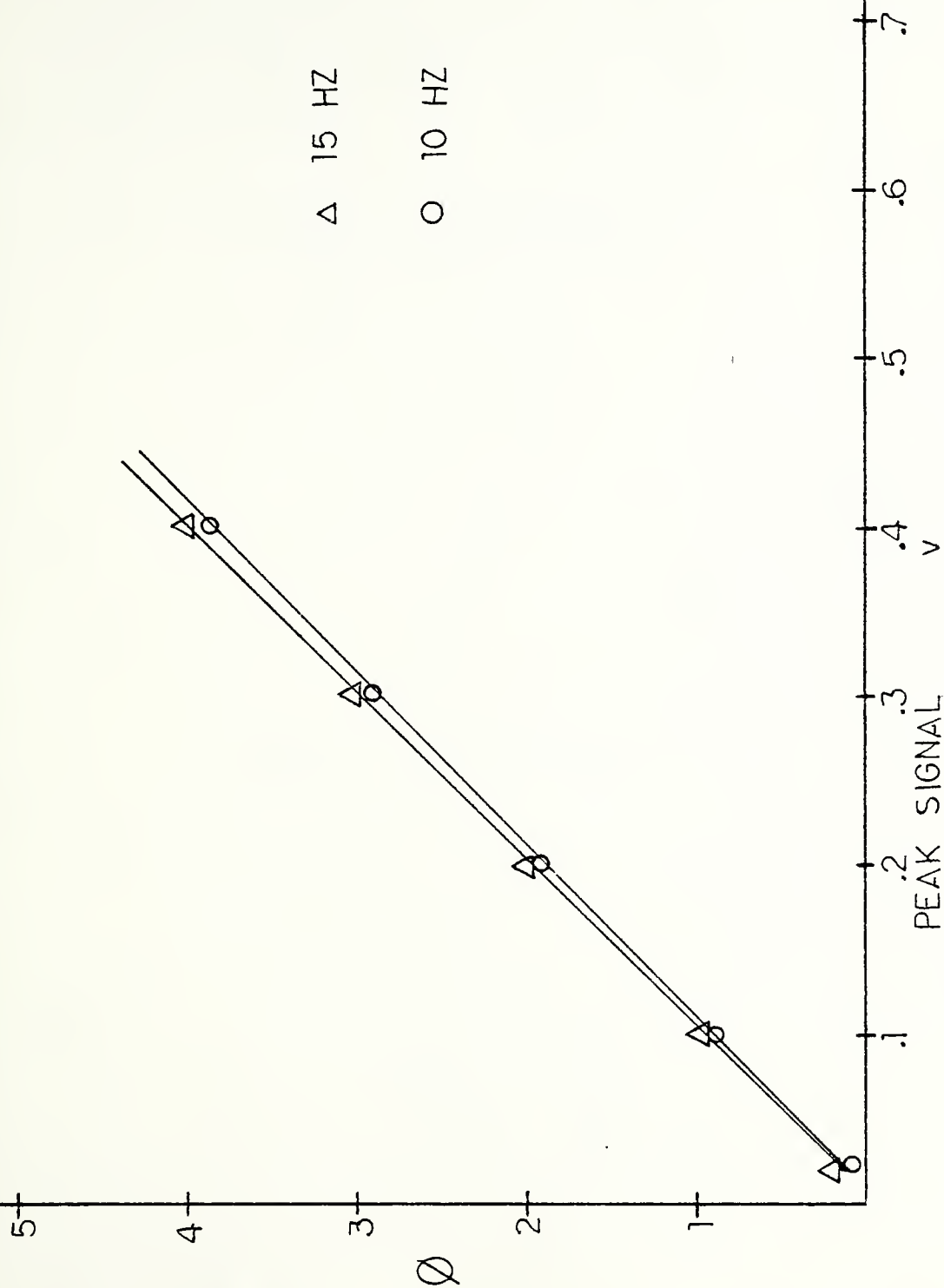


FIG. (7) Type (ii) Mirror Frequency Response



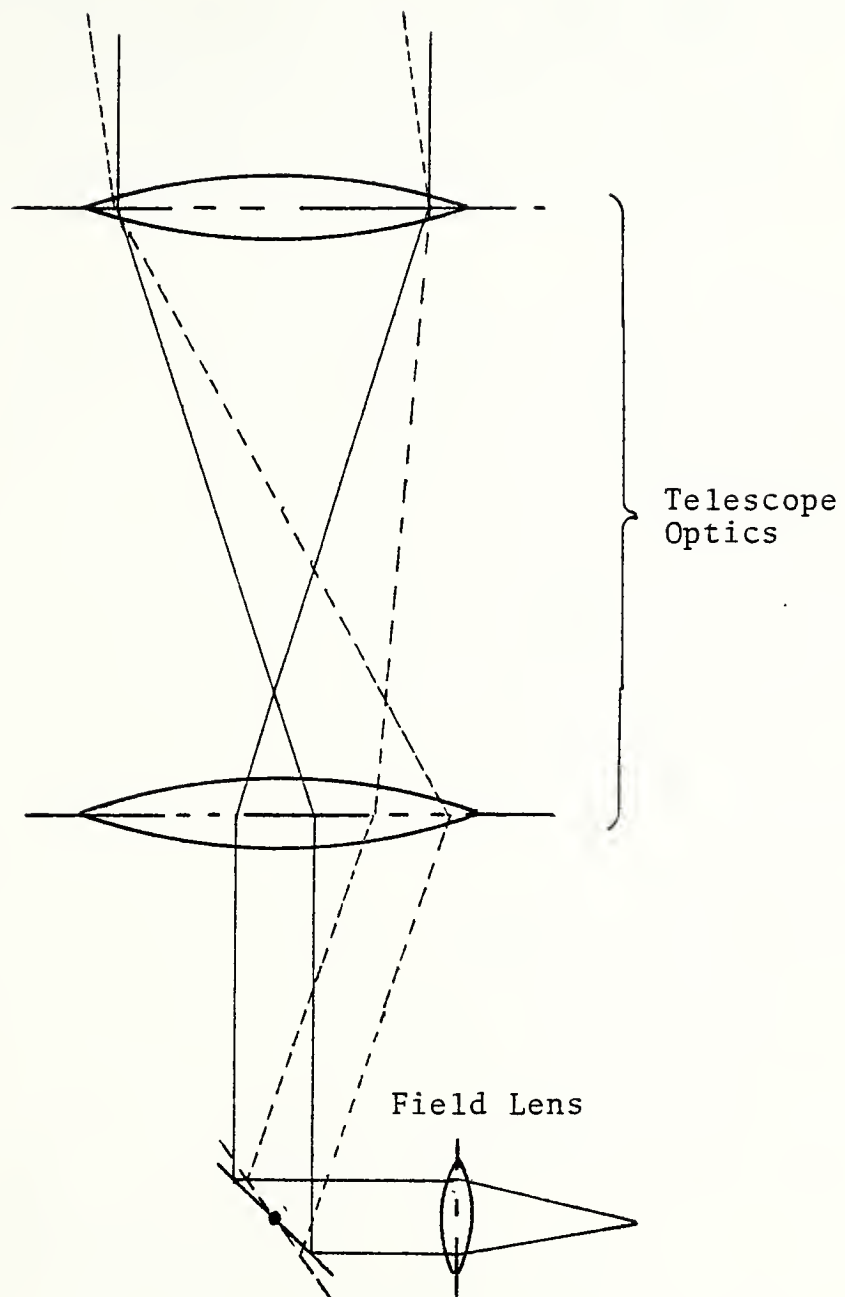


FIG. (8) "Parallel" Beam Scanning System



in FIG. (9). While much simpler to construct and align, convergent beam scanners cause image deformation by mirror induced focal point shifting as shown in FIG. (10).

The first design used the parallel beam scan technique. It quickly became apparent that alignment of the system would be tedious and unproductive. Two considerations prompted a switch to the simpler convergent beam scanner.

First, to allow rapid scan speeds, the two attached mirrors had to be small due to inertia considerations. The type (i) is a circle 2.54 cm in diameter and the type (ii) a rectangle with dimensions 3.3 cm by 3.94 cm. With the Dahl-Kirkham exit beam aperture diameter equal to 3.2 cm, and both mirrors stationary positions being at 45 degrees in relation to the exit beam, the mirror motions must be kept small in order that they present a sufficient cross section to the image beam.

Secondly, the Dahl-Kirkham telescope has a 25.4 cm back focal length for an object at infinity as measured from the primary mirror. If the scanning system could be located close to the exit aperture, it would be (due to the long back focal length) operating in a region where the image beam was nearly parallel.

Because of the necessity for small mirror motions and the long focal length, the use of the convergent beam technique would not cause unacceptable image blur through beam defocus. Consequently, the convergent beam scan system was settled upon as the system for the FLIR.



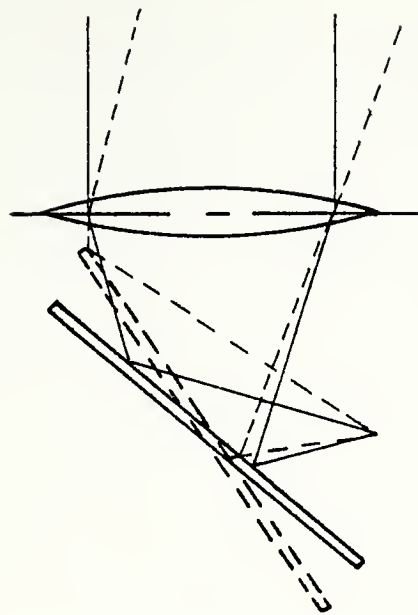


FIG. (9) Convergent Beam Scanning System

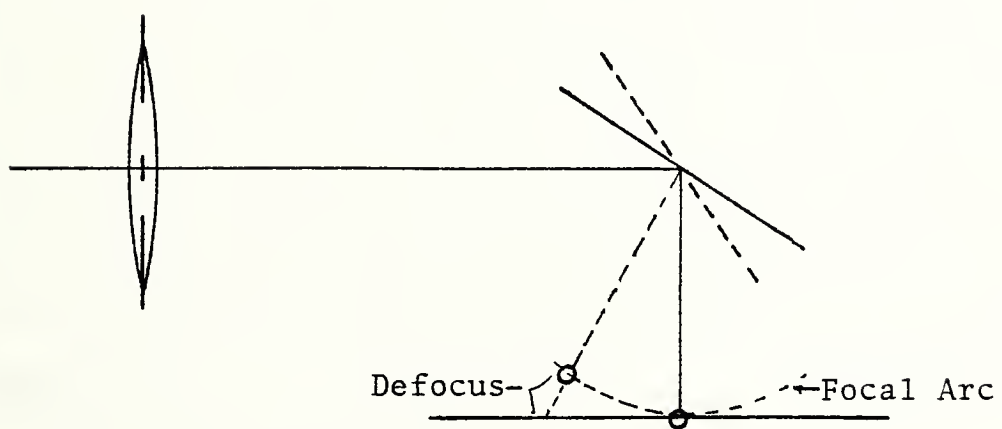


FIG. (10) Convergent Scan Defocusing



## 2. Raster

The raster consists of two orthogonal linear motions. The high speed scan is fixed near its maximum value for linear sinusoidal frequency response. The fast scan is set at 200 Hz in an asymmetrical sawtooth pattern.

E. W. Engstrum, Ref (2), in a study of television characteristics, concluded that the ratio of lines per picture height has a definite impact on visual acceptability. He found that a ratio of 240 lines per picture is satisfactory, 180 lines is marginal, 120 lines barely acceptable while 60 lines is totally inadequate. Given a fast scan rate of 200 lines per second, to optimize the raster at greater than 240 lines per picture means that the slow scan must have at least a 1.2 second interval excluding flyback time. This value being well within the capability of the slow scan mirror was set to a value of 1.5 seconds with a flyback time of .5 seconds. This is proportional to a .5 Hz frame rate and 300 lines per picture height. As with the fast scan, an asymmetrical sawtooth is used. This was one area where the human/machine interface was amenable to optimization.

While it is undesirable for the operator to perceive the raster, it is visible on the screen as a line which slowly moves down the screen, painting the video picture.



### C. DETECTORS

Any consideration of detectors must first start with a decision as to the particular wavelengths to be covered. For military FLIRs, the regions 3-5  $\mu\text{m}$  and 8-12  $\mu\text{m}$  are of particular interest. However, to simplify alignment and speed the design process, the first wavelengths investigated were in the visible.

State-of-the-art FLIRs use linear arrays with full field planar arrays still in the future. Fortunately, the two single cell detectors, manufactured by Santa Barbara Research, Inc., were modern, high detectivity and fast response-time detectors. They consist of a Mercury Cadmium Telluride (HgCdTe) and an Indium Antimonide (InSb) detector having circular dimensions of 2 mm. They are mounted in side-looking dewars and utilize liquid nitrogen cooling to 77°K. The dewars are capable of a minimum of four hours nitrogen hold time. The HgCdTe detector operates in the 8-14  $\mu\text{m}$  region and is equipped with an IRTRAN 2 window. The InSb (PV) detector operates in the 3-5  $\mu\text{m}$  band and is equipped with a sapphire window. Figures (11) and (12) show some of the IR detectors' operating characteristics.

In the visible range, a silicon avalanche diode is used. It has a range out to approximately 1.1  $\mu\text{m}$  as shown in FIG. (13).



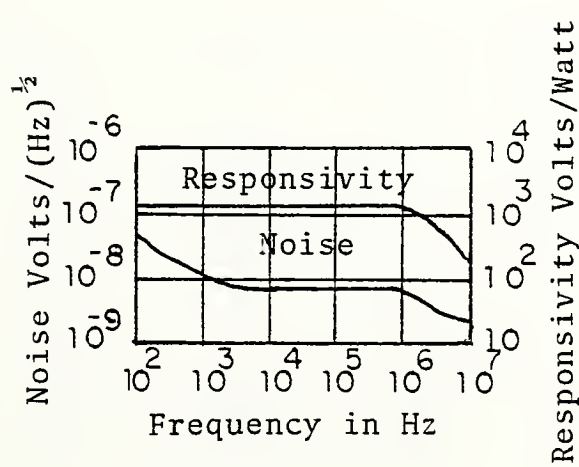
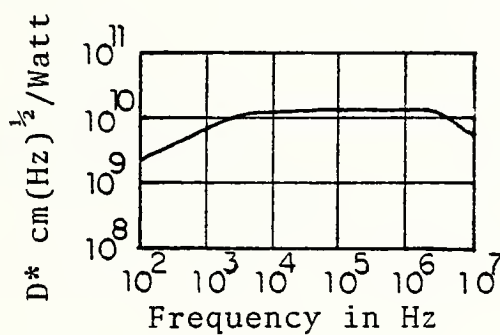
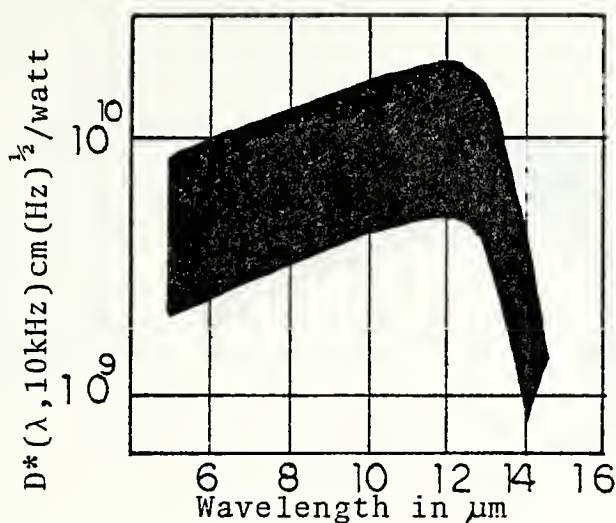


FIG. (11) HgCdTe Detector Characteristics



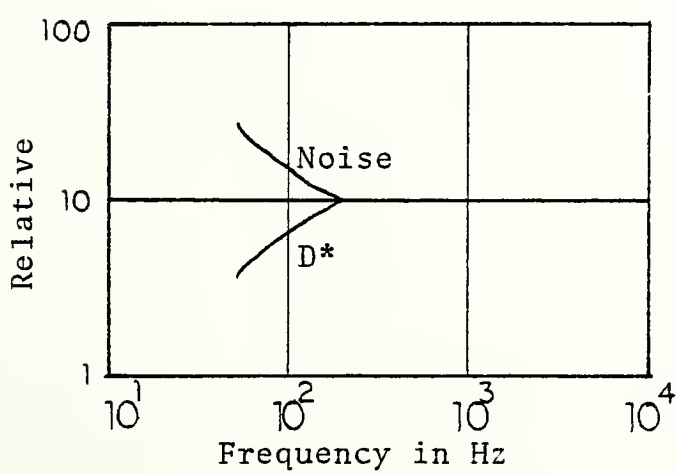
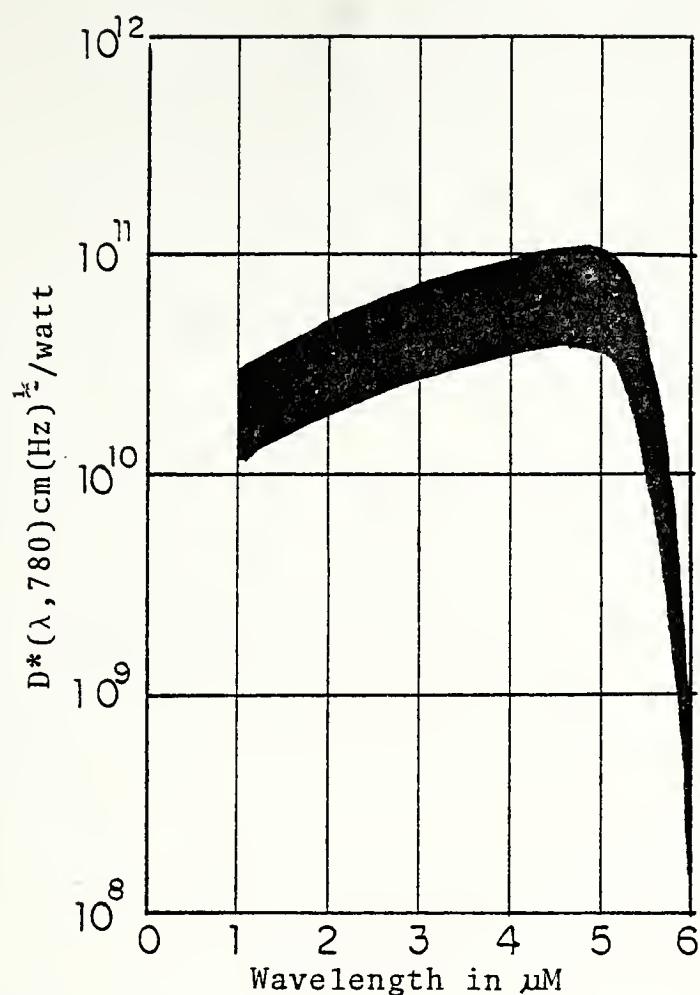


FIG. (12) InSb Detector Characteristics



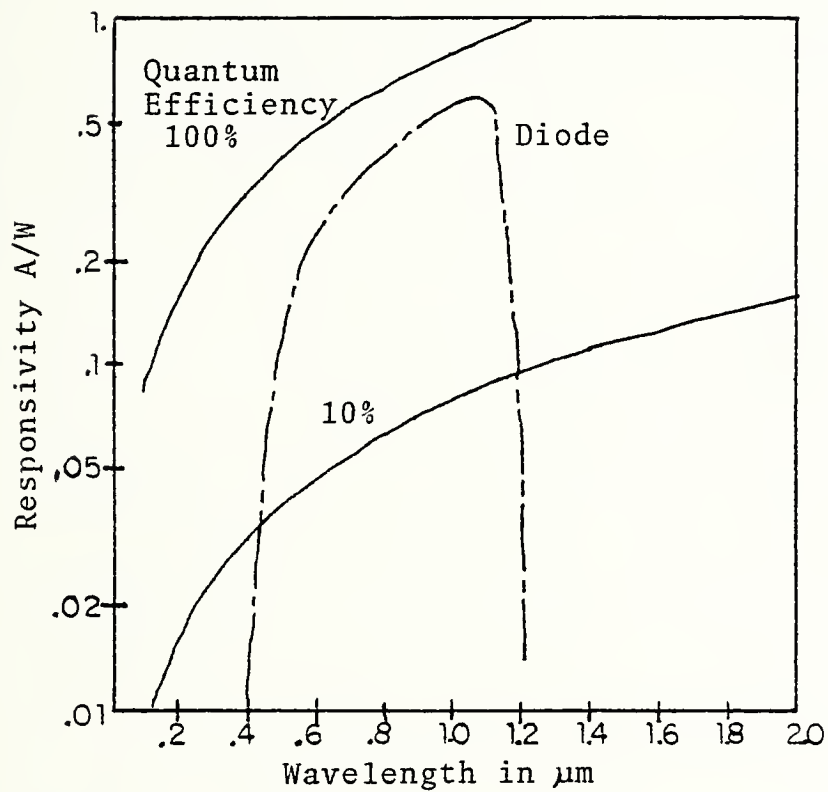


FIG. (13) Silicon Avalanche Diode Characteristic



The angular projection of a detector with dimension,  $a$ , through an optical system with an effective focal length,  $f$ , is:

$$d = a/f$$

When using a focal plane baffle, the quantity,  $a$ , becomes the exposed detector dimension. Reducing the detector size reduces the instantaneous field of view and thus increases the resolution of the system. A smaller detector size also reduces the random detector noise, thus increasing the signal to noise ratio, provided that the background radiation noise is dominant.

Reference 3 describes a commercial, single-cell detector FLIR which uses a circular detector with a diameter of .005 cm. Utilizing this as a target dimension, the three detectors with 2 mm diameter dimensions have surfaces 40 times larger than desired. The larger dimensions, while simplifying alignment, reduce the resolution of the system. Two possible methods for decreasing detector size are (i) smaller active area of detector or (ii) occluding most of the large detector active area with a baffle. The latter method was chosen, and small pinholes, using a #80 drill, were manufactured and positioned over the center of each detector. A #80 drill, the smallest commercially available, has a diameter of .0343 cm and while this is still seven times larger than the targeted .005 cm, it is acceptable.

Another factor which has to be considered with the detectors is the response time in relation to scan speed.



The dwell time of a single cell detector in a scanning system is given by:

$$T_d = \frac{\sigma}{AF}$$

where:  $\sigma$  = one dimensional instantaneous field of view  
A = one dimensional total field of view  
F = 1/Tf  
Tf = single line scan time  
Td = dwell time

For the system:

$$\begin{aligned}\sigma &= .15 \text{ milliradians} \\ A &= 13 \text{ milliradians} \\ F &= 200 \text{ 1/sec} \\ T_d &= 58 \text{ usec}\end{aligned}$$

HgCdTe has a response time of 100-800 nsec and InSb has a response time of approximately 1 usec. With the dwell time a minimum of 58 times longer than the slowest response time there are no problems in this area.

#### D. ELECTRONICS

The major thrust of the electronics suite was to keep it as simple as possible while still providing the necessary services for the optical portions of the system.

The electronics package is broken down into two sections: mirror scan drive and detector/video support. The mirror scan drive section provides drive power signals to the mirrors and scan control signals to the video system.

##### 1. Mirror Scan Drive

A Wavetech function generator provides two asymmetric sawtooths to generate the raster. In addition, it



generates a control pulse which is used for video flyback blanking. TABLE (II) lists all the components of each area.

The raster signals are fed to a synchro control unit and a power amplifier which provide drive power to the mirrors. The fast scan mirror, due to its feedback control system, requires a special scanner control unit while the slow scan mirror utilizes a HP 467A DC power amplifier.

The response of the mirrors to the raster signal has an inherent time delay. In an attempt to avoid this lag interfering with proper synchronization between video signal and video raster, the fast scan signal for the video is taken from the position feedback signal from the fast scan mirror. This signal is available at the synchro scanner control. This type of position signal is not available with the slow scan nonfeedback mirror, so that the slow scan raster signal comes from the HP 467A DC amplifier.

<u>EQUIPMENT</u>	<u>USE</u>
<u>Mirror Support</u> Wavetech Model 184 Function Generator	Raster Control
General Scanning CCX101 Scanner Control	Fast Mirror Drive
Hewlett Packard 467A Power Amp.	Slow Mirror Drive
<u>Detector/Video Support</u> Interstate Elect. Corp. P12 Pulse Generator	Flyback Blanking

(cont.)



<u>EQUIPMENT</u>	<u>USE</u>
Princeton Applied Research Model 113 Preamp	Detector Signal Amp.
Hewlett Packard 465A Power Amp.	Video Signal Amp.
Hewlett Packard 467A Power Amp.	Blanking Signal Amp.
Monsanto OS-226 (P)/USM-368 Oscilloscope	Display

TABLE (II) FLIR Electronic Equipment

## 2. Detector/Video

In the video section, the most important component is the display unit. The display unit has to be able to utilize adjustable scan signals in two dimensions and be capable of beam intensity modulation. In addition, the screen has to have a fairly long decay phosphor to compensate for the slow frame time. The oscilloscope listed in TABLE (II) meets all these requirements nicely.

To obtain useable signals from the detectors, each requires different biasing and/or power supply arrangements. The InSb (PV) detector is operated into a 300 MegOhm input resistance around a bias voltage of 0; FIG (14). The HgCdTe detector is photoconductive, which means a conduction current is necessary, while the avalanche photodiode operates near breakdown and requires 156 volts. Figure (15), (16), and (17) detail the requisite circuits.



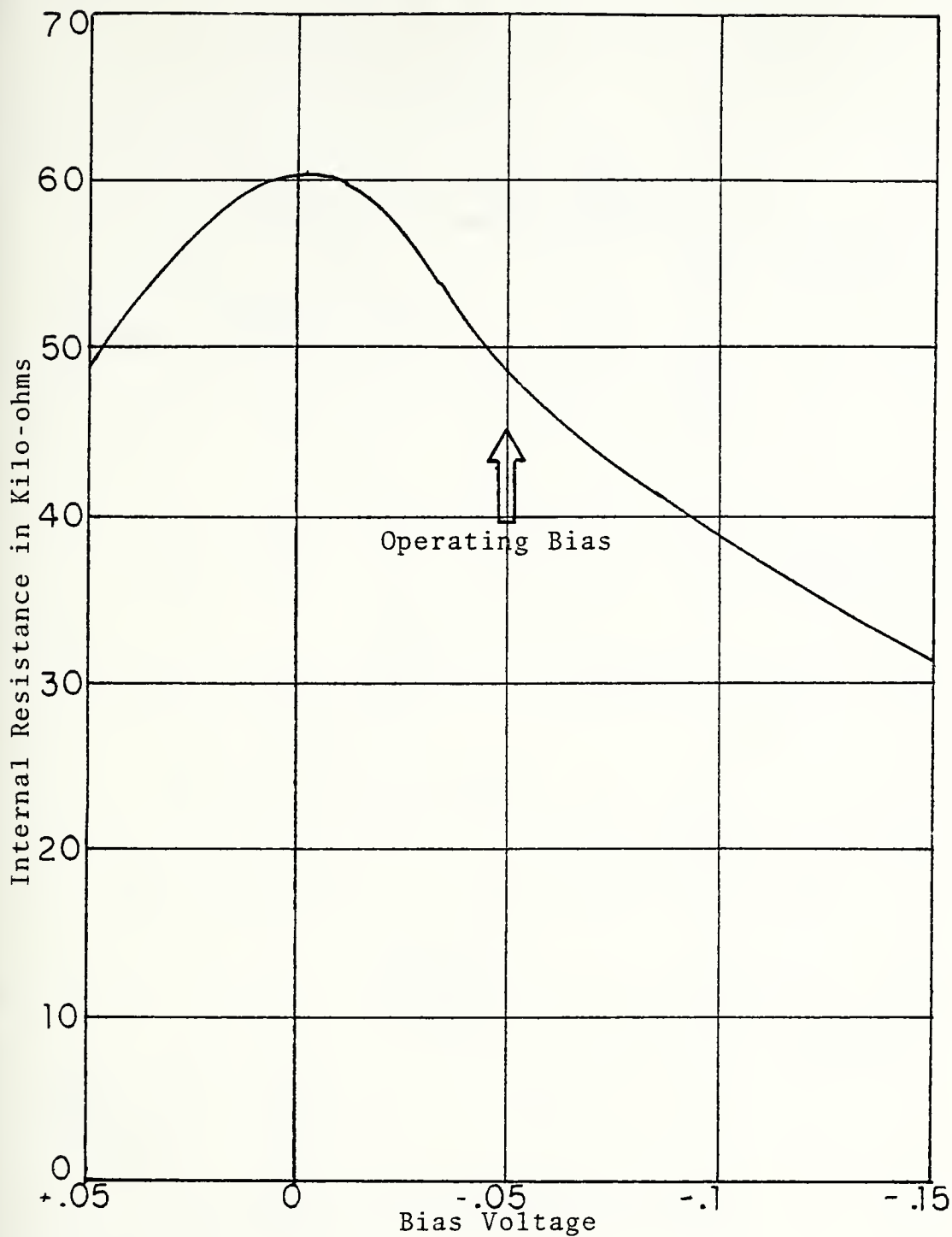


FIG. (14) Internal Resistance as a Function of Bias Voltage for the InSb Photovoltaic Cell



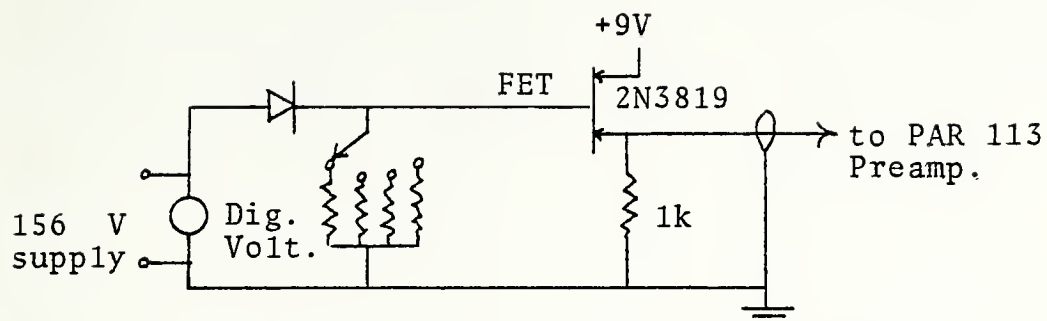


FIG. (15) Circuit for Avalanche Detectors

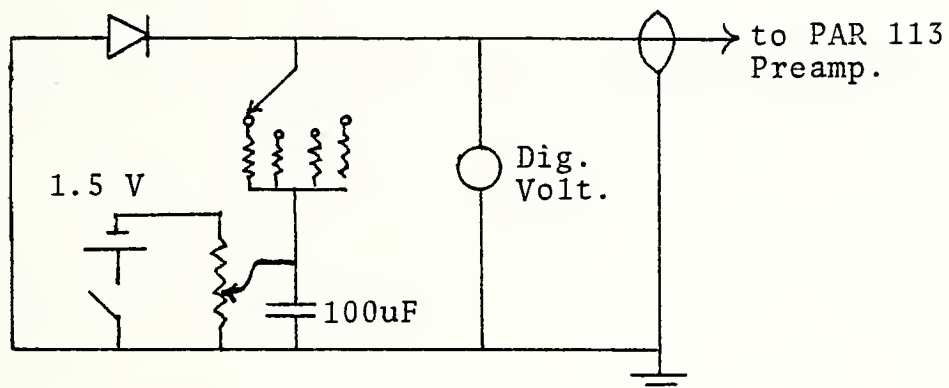


FIG. (16) Circuit for InSb Photovoltaic Cell

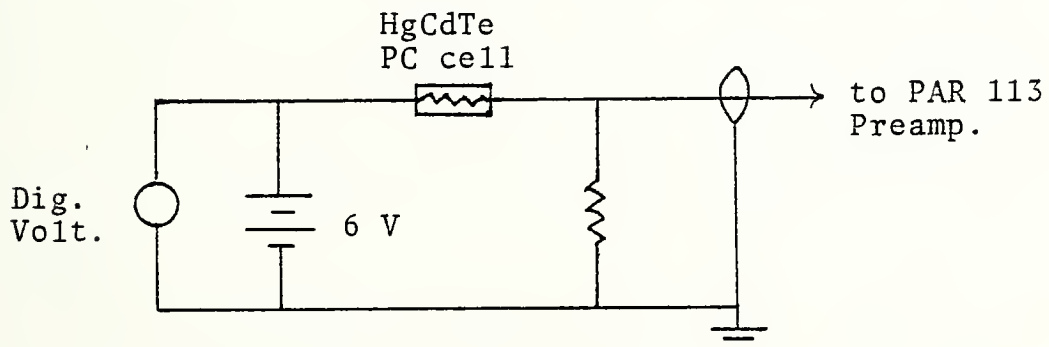


FIG. (17) Circuit for HgCdTe Photoconductive Cell



All three detector outputs are fed into a PAR 113 high gain preamp which normally would provide all the necessary amplification. However, the fact that the signal is required to modulate the beam intensity for the oscilloscope means that an additional stage of amplification is necessary. The second stage of amplification is accomplished by a HP 465A DC power amplifier which can provide 40 db of gain to comparatively high voltage levels without saturation.

To provide for a more acceptable video display, the screen is blanked during the slow scan flyback time. Only the slow scan flyback is blanked; the fast scan flyback does not cause any noticeable interference.

Blanking is accomplished by a pulse generator triggered from the function generator, which then outputs a single pulse of the proper dimensions. Since the oscilloscope operates on the principle that a negative voltage is proportional to the brightness level, the pulse generator has to produce a positive pulse. For the Monsanto Oscilloscope a minimum voltage of +10 volts is required to cause blanking.

Due to impedance mismatching at the oscilloscope Z input, a diode was inserted between the HP 467A and the Z input junction. The diode allows the pulse to pass while preventing signal loss to the pulse generator from the HP 465A signal amplifier. The HP 467A pulse generator



amplifier was added to increase the blanking pulse's amplitude. This is required because the pulse generator is capable of a maximum pulse amplitude of 10 volts and it is attenuated by the diode below useable levels.



#### IV. RESULTS

##### A. VISIBLE

After ensuring that the individual subsystems operated properly, they were integrated into the FLIR system. As discussed previously, the first imaging attempts took place using the silicon avalanche photodiode in the visible region.

Figure (18) shows the target for the first imaging attempts. It was located at the end of a passageway, 132 m from the system. Initial scene illumination was one 100 watt incandescent light bulb.

Utilizing a ground-glass screen, and slowing down the fast scan mirror, allowed the field of view to be measured. At 132 meters the field scanned was 83.8 cm by 38.1 cm which is proportional to a 6 milliradian by 3 milliradian field of view. Normal mirror scan frequencies during this time were 160 Hz and 3 Hz.

Figure (19) shows the first recognizable video image produced by the system. It is the 100 watt light bulb and its white reflector, which had been turned to shine directly toward the telescope, seen through the vertical slats of a wooden chair. In this case, the detector was fitted with a .034 cm pinhole.



Thesis  
G86095  
c.1

Gruber

Experimental FLIR  
study.

183933

thesG86095  
Experimental FLIR study.



3 2768 002 13572 5  
DUDLEY KNOX LIBRARY